TUNABLE AND SELF-REINFORCED POLYETHYELENE/MCM-41 NANOCOMPOSITES BY *IN-SITU* POLYMERIZATION

M. Rosário Ribeiro[1], João M. Campos[1], A. Bento[1], João P. Lourenço[2], Ernesto Pérez[3] and María L. Cerrada[3]

[1]Instituto Superior Técnico - Universidade Técnica de Lisboa. Av. Rovisco Pais 1, 1049-001 Lisboa, Portugal
[2]Faculdade de Ciências e Tecnologia-Universidade do Algarve. Campus de Gambelas, 8005-139 Faro, Portugal.
[3]Instituto de Ciencia y Tecnología de Polímeros (CSIC). Juan de la Cierva, 3, 28006, Madrid, España.

Introduction

Zeolites and mesoporous materials are of particular interest to be used as inorganic phase for the preparation of multicomponent polymeric nanocomposites. They present stable 3D framework structures that may lead to some interesting confinement effects and that can resist to the forces produced by intercalated polymers. There are two primary methods for attainment of nanocomposites from porous inorganic materials [1]: (i) direct threading of preformed polymer through the inorganic host channels (soluble and melting polymers), usually limited by the size, conformation and diffusion behavior of the polymers, and (ii) the in-situ polymerization in the pores and channels of the inorganic hosts. In-situ polymerization is supposed to lead to better filler dispersion than simple melt preparation, especially at high filler contents, and provides a promising strategy for obtaining nanocomposites with desirable properties. Our interest is now primarily focused on preparation of hybrids based on polyethylene (HDPE) and meso-structured MCM-41 due to the great importance of this polymer in different application fields. Therefore, several methodologies for preparation of this type of nanocomposites are currently being explored in our group aiming to improve interfacial contact between the MCM-41 and the matrix.

A set of HDPE nanocomposites are then synthesized and characterized using MCM-41 in a double role (1) carrier for the immobilization of the polymerization catalysts and allowing ethylene polymerization within its pores and channels and as (2) inorganic nanofiller of the polyethylene matrix formed. The content of inorganic component analyzed ranges from 0 to around 30 weight percentage. This route allows us gaining some knowledge on the potential offered by these hybrid inorganic/organic materials.

On the other hand, the enhancement of compatibility of both components will permit the use of lower inorganic content and, accordingly, a composition of about 10 wt. % is explored when distinct methods incorporating 10-undecenoic acid (UEA) as interfacial agent are evaluated. These protocols involve: (1) the use as filler of MCM-41 modified with UEA in a homogeneous polymerization; (2) homogeneous copolymerization of ethylene with UEA in presence of MCM-41 as filler; and (3) modification of MCM-41 with UEA and its use as filler and as catalyst carrier in the further polymerization.

Accordingly, the aim of this investigation is, on one hand, to extensively characterize the morphological and mechanical behavior found in hybrid PE/MCM-41 nanocomposites prepared in a wide range of composition and without the use of interfacial agent and, on the other hand, to check some mechanical parameters (basically microhardness and storage modulus) in nanocomposites at a given MCM-41 content (around 10 wt. %) synthesized using different routes for improving interfacial adhesion between the two components.

Experimental

Preparation of family of hybrid PE/MCM-41 nanocomposite materials with MCM-41 contents ranging from 0 to around 30 wt. % were performed as described in reference [2].

The hybrid nanocomposites, labeled as HDPE/MCM-41(*x*) -x being the weight content in MCM-41-, were obtained as thick films (around 400 μm) by compression molding in a Collin press between hot plates at 170 ºC, at a pressure of 1.5 MPa, for 5 min. Each of the HDPE/MCM-41(x) specimens was crystallized by a fast quench in cold water after its melting in the press.

The wide, middle and small angle X-ray synchrotron studies (WAXS, MAXS and SAXS, respectively) were performed in the soft-condensed matter beamline A2 at Hasylab (Hamburg, Germany), working at a wavelength of 0.150 nm, at a heating rate of 8 °C/min and acquiring profiles every 15 s.

TEM images were obtained in Hitachi H8100 equipment. Nanocomposite samples were deposited in a Cu/polymer grid sample holder.

Calorimetric analyses were carried out in a Perkin-Elmer DSC7 calorimeter, connected to a cooling system and calibrated with different standards. The sample weights ranged from 5 to 7.5 mg. A temperature interval from -50 ºC to 150 ºC has been studied and the used heating rate was 10 ºC/min. For crystallinity determinations, a value of 290 $\tilde{J}g^{-1}$ has been taken as the enthalpy of fusion of a perfectly crystalline material [3].

The weight loss was estimated by thermogravimetry using a TA Instruments TGA Q500 equipment working under an inert atmosphere. The equipment was calibrated according to standard protocols. The

sample weights ranged from 4 to 6 mg, and the heating rate was 10ºC min^{-1}.

Viscoelastic properties were measured in a Polymer Laboratories MK II dynamic mechanical thermal analyzer working in a tensile mode. The complex modulus and the loss tangent for each sample were determined at 1, 3, 10 and 30 Hz over a temperature range from -150 to 130 ºC, at a heating rate of 1.5 ºC min^{-1}.

A Vickers indentor attached to a Leitz microhardness tester was used to perform microindentation measurements undertaken at 23 ºC. A contact load of 0.98 N and a contact time of 25 s were employed. Microhardness, MH, values (in MPa) were calculated according to the relationship [4]:

$$MH = 2 \sin 68^\circ P / d^2 \qquad (1)$$

where P (in N) is the contact load and d (in mm) is the diagonal length of the projected indentation area. Diagonals were measured in the reflected light mode within 30 s of load removal, using a digital eyepiece equipped with a Leitz computer-counter-printer (RZA-DO).

Results and Discussion

The zirconocene catalyst was immobilized on the MCM-41 via a direct impregnation route. Different MCM-41-based supports and polymerization conditions have been carefully selected to control the activity level and to, consequently, enable the preparation of hybrid nanocomposite materials with different contents in inorganic nanofillers (from 3 to 28% wt. %) [2].

We expect that MCM-41 aggregates can be dispersed, in a certain extent, during the experimental procedure to prepare these nanocomposites. Information about their distribution and their size within the polyethylene matrix has been obtained by TEM. Figure 1 shows that filler particles are uniformly dispersed within the polyethylene matrix although some aggregates are observed. However, their average sizes are at the nanometric scale as seen in this picture for the HDPE/MCM-41(14) nanocomposite.

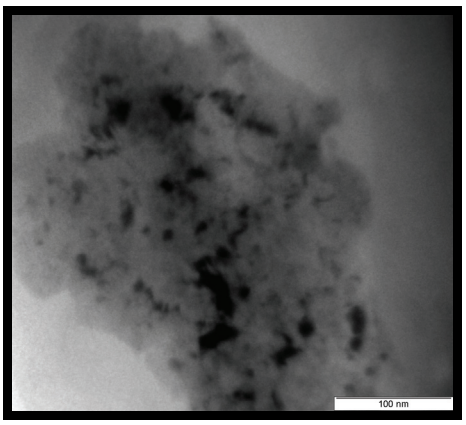

Figure 1. TEM micrograph of the HDPE/MCM-41(14) nanocomposite.

X ray results indicate several characteristics of these novel polymeric-based materials. From wide angle region, it can be deduced that HDPE and all of the HDPE/MCM-41(*x*) nanocomposites exhibit an orthorhombic crystal lattice and crystallinity at room temperature do not vary much with incorporation of MCM-41. From the region of middle angles it is seen that the different nanocomposites present at room temperature the same diffractions than the initial MCM-41 materials indicating that the long-range regular hexagonal structure is retained after polymerization. However, differences in intensity and width are found for the various samples if comparison with neat MCM-41 is performed. The first observation results from the fact that MCM-41 is not the major component in the nanocomposite, the diffraction peak intensity increasing as MCM-41 content does. The second one is ascribed to the presence of polyethylene chains within the pores and channels of MCM-41, slightly deforming the original well-ordered long-range structure.

The results obtained from the small angle interval indicate that position of the SAXS peak is moved to lower 1/d values, *i. e.*, to longer long spacings (L = d) as MCM-41 content is increased, as depicted in Figure 2. Therefore, HDPE/MCM-41(*23*) and HDPE/MCM-41(*28*) nanocomposites, although they are semicrystalline materials as observed from WAXS and DSC results, do not show any peak since the maximum has been displaced out of the empirical scale.

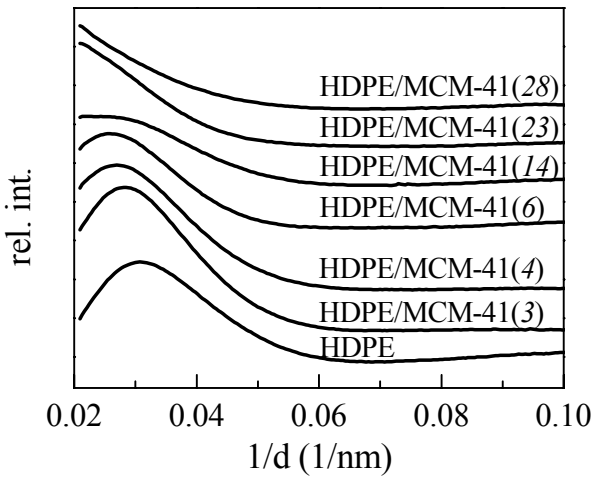

Figure 2. Small angle X ray diffraction patterns at room temperature.

Additional knowledge on the structure developed in these nanocomposites is obtained from their thermal properties. The DSC first melting curves for all of specimens indicate that when the enthalpy is normalized, taking into account the actual amount of HDPE within the hybrid materials, the values obtained are rather similar for the neat HDPE and the nanocomposites, as reported in Table 1. On the other hand, the DSC melting temperatures do also remain practically unaffected in the different nanocomposites compared to that exhibited by HDPE. These DSC

results are in good agreement to those derived from the melting WAXS synchrotron real-time measurements. The crystallization exotherm shows a significant diminishment of crystallinity after normalization and, in addition, a slight increase in crystallization temperature is observed for those nanocomposites with the highest MCM-41 contents. This behavior seems to point out that crystallization is postponed by the presence of mesoporous inorganic solid. Accordingly, crystallization of intercalated HDPE located within MCM-41 channels in the nanocomposites seems to be extremely hindered because of a confinement effect leading to the delay of the tri-dimensional ordering.

Polymer Sample	f_c^{XR}	L (nm)	f_{cm}^{DSC}	T_m^{DSC} (ºC)	T_c^{DSC} (ºC)	f_{cc}^{DSC}
HDPE	0.51	32.5	0.53	132	117	0.56
HDPE/MCM-41(3)	0.54	35.6	0.52	131	117	0.55
HDPE/MCM-41(4)	0.55	37.1	0.53	133	117	0.54
HDPE/MCM-41(6)	0.54	38.4	0.53	132	118	0.55
HDPE/MCM-41(14)	0.54	39.7	0.55	132	119	0.49
HDPE/MCM-41(23)	0.54	-	0.55	132	120	0.40
HDPE/MCM-41(28)	0.53	-	0.51	132	121	0.34

Table 1. Normalized crystallinity estimated from X ray profiles, f_c^{XR}, long spacing values determined from SAXS patterns, L, and crystallinity degree on melting and cooling DSC experiments, f_{cm}^{DSC} and f_{cc}^{DSC} together with melting and crystallization temperatures, T_m^{DSC} and T_c^{DSC}, respectively.

Other interesting aspect is related to the results obtained from thermogravimetry, as seen in Figure 3. The beginning of degradation is shifted to lower temperature as MCM-41 content increases in the nanocomposites. Moreover, the derivative curves, represented on the bottom, prove that degradation process takes place in a unique stage for the neat polymeric matrix and the nanocomposites with low MCM-41 incorporations whereas an overlapping of two stages is seen as content is raised, one probably related to the polymer inside the channels and the other to those macrochains surrounding the fillers. All these features can be ascribed to a catalytic effect of MCM-41 in the degradation process of PE. A similar effect has been found by Marcilla et al. [5] when studying the degradation of PE under N_2, in the presence and absence of mesoporous MCM-41, by thermogravimetric analysis (TGA). Aguado et al. [6] have also shown the efficiency of mesoporous aluminosilicate MCM-41 as promoter towards degradation of polyolefins into liquid fuels. Nowadays, this might be quite interesting in relation to the degradation of these polyolefins into basic petrochemicals as feedstock or fuel for downstream processes after their life service, making these self-reinforced polyolefinic materials environmentally welcome and with an added value.

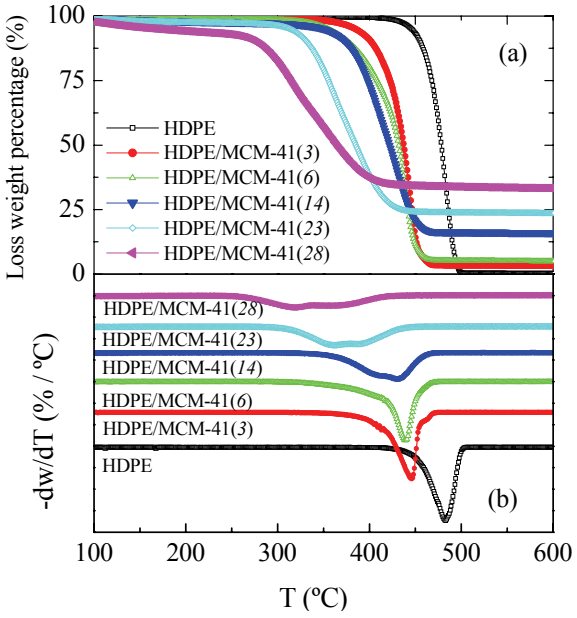

Figure 3. (a) TG and (b) DTG curves of different nanocomposites. DTG curves have been vertically shifted for clarity.

Figure 4 shows the variation of the storage modulus for the different nanocomposites. An increase of this parameter is seen as MCM-41 content does. Crystallinity is rather similar in the different specimens whereas crystal thickness increases as MCM-41 nanofiller content rises. Therefore, the stiffness enhancement observed in the nanocomposites can be ascribed to both the larger size of crystallites and the inherent reinforcement effect of nanofiller. This rigidity increase with MCM-41 composition is more significant at temperature above the ambient one, as observed in Figure 4, *i.e.*, when mobility within the olefinic polymer rises. This fact is rather interesting from a practical standpoint since these materials exhibit improved mechanical characteristics without varying the final processing temperature (T_m is practically constant for all of the specimens).

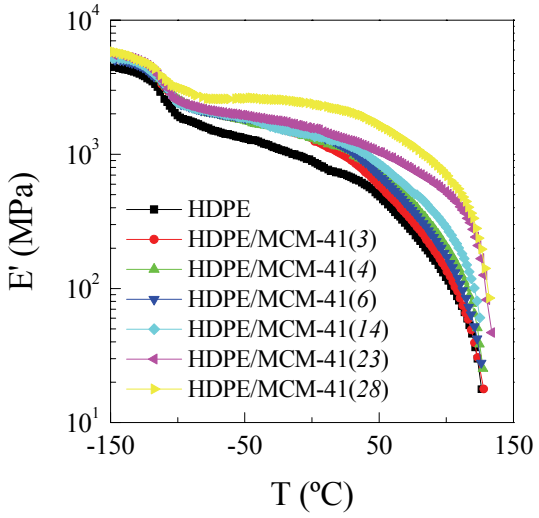

Figure 4. Temperature dependence of storage modulus for the different HDPE/MCM-41(*x*) nanocomposites.

This increase in rigidity is also found from microhardness determination, as seen in Figure 5. This type of test is very useful because its magnitude correlates rather well with elasticity modulus if material is homogeneous, as also depicted in Figure 5. Moreover, it is a rather fast method requiring a relatively small amount of material.

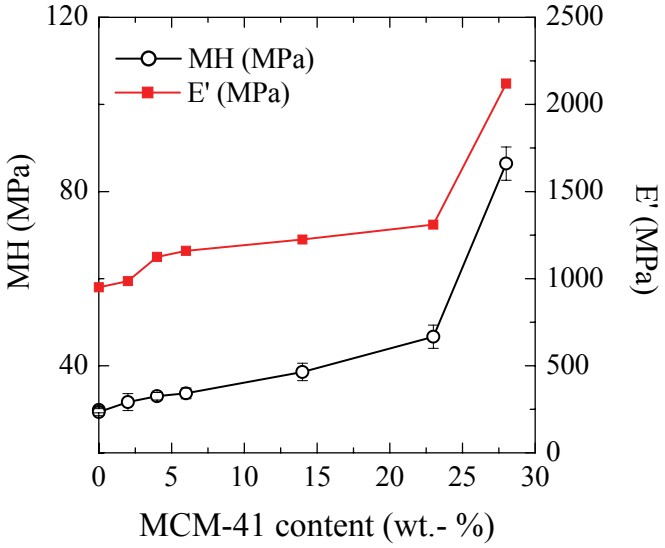

Figure 5. Dependence of microhardness (MH, left Y axis) and storage modulus (E', right Y axis) on MCM-41 content within the nanocomposites.

The good relationship between microhardness and other bulk mechanical properties related to stiffness, as aforementioned, has been an important aspect to be considered in order to evaluate preliminary the effect on final properties of modifying the MCM-41 particles or the HDPE matrix with 10-undecenoic acid. Its incorporation, in principle, should lead to an enhancement of the mechanical performance because of a better interfacial contact and, accordingly, a better stress and strain transfer between the two components. The microhardness values obtained for the different methods seem to confirm this assumption. The most promising strategies will be presented and discussed along the lecture.

In conclusion the novel HDPE/MCM-41 self reinforced nanocomposites present a very high potential in terms of mechanical parameters and sustainable features.

Acknowledgements

Financial support of Fundação para a Ciência e a Tecnologia (FCT), (Projecto PDCT/CTM/66408/2006) and Ministerio de Educación y Ciencia (project MAT2007 65519-C02-01) is acknowledged. J.M.C. thanks the FCT for his PhD scholarship (ref. SFRH/BD/16547/2004). The synchrotron work was supported by the European Community - Research Infrastructure Action under the FP6 "Structuring the European Research Area" Programme (through the Integrated Infrastructure Initiative "Integrating Activity on Synchrotron and Free Electron Laser Science"), contract RII3-CT-2004-506008 (IA-SFS). We thank the collaboration of the Hasylab personnel in the soft-condensed matter beamline A2, especially Dr. S. S. Funari.

References

1. Kickelbick G. Concepts for the incorporation of inorganic building blocks into organic polymers on a nanoscale. *Prog. Polym. Sci* .**28** (2003), 83-114.
2. Campos J. M., Lourenço J. P., Ribeiro M. R., and Fernandes A. Ethylene polymerisation with zirconocene supported in Al-modified MCM-41: Catalytic behaviour and polymer properties. *J. Mol. Catal. A-Chem.*, **277** (2007), 93-101.
3. Quinn F. A. and Mandelkern L. Thermodynamics of crystallization in high polymers - poly-(ethylene). *J. Am. Chem. Soc.* **80** (1958), 3178-3182.
4. Baltá-Calleja F. J. Microhardness relating to crystalline polymers. *Adv. Polym. Sci.*, **66** (1985), 117-148.
5. Marcilla A., Gómez-Siurana A., Menargues S., Ruiz-Femenia R. and García-Quesada J. C. Oxidative degradation of EVA copolymers in the presence of MCM-41. *J. Anal. Appl. Pyrolysis*, **76** (2006), 138.
6. Aguado J., Serrano D. P., Romero M. D. and Escola J. M. Catalytic conversion of polyethylene into fuels over mesoporous MCM-41. *Chem. Commun.*, **6** (1996), 725-726.